**HYDROTHERMAL CLAY MINERAL PRODUCTION IN METEORITE IMPACTS: LESSONS FROM $\delta^2$H AND $\delta^{18}$O OF SMECTITES FROM THE CHICXULUB PEAK-RING.**

S. L. Simpson, G. R. Osinski, F. J. Longstaffe. Centre for Planetary Science and Exploration/Dept. of Earth Sciences, The University of Western Ontario, London, Canada (SSimps56@uwo.ca).

**Introduction:** Initial lithologic characterization of core material recovered from the 2016 joint International Ocean Discovery Program (IODP)-International Continental Scientific Drilling Program (ICDP) Expedition 364 has produced exemplary evidence for post-impact hydrothermal alteration of the Chicxulub peak-ring [1–4]. The impact melt-bearing breccias and melt rocks of the upper peak-ring are pervasively altered and preserve a diverse suite of clay minerals and zeolites, in addition to carbonates, sulfides and other phases. The conditions under which these minerals form within impact settings on both Earth and Mars remains unclear due, in part, to a lack of detailed studies of terrestrial craters, and the large range of possible conditions that could lead to their development. Additional geochemical and isotopic datasets are needed to provide environmental constraints, particularly for such phases present on the surface of other terrestrial bodies (e.g., Mars), for which there is often minimal to no geologic context. Clay minerals, in particular, remain prime exploration targets on other terrestrial planets as they form in the presence of water and preserve information on fluid chemistry and temperature. Clays with high surface to volume ratios and cation exchange capacity (CEC) (i.e. the smectite group) can also act as templates for prebiotic organic materials synthesis [5–7].

Here we present the first $\delta^2$H and $\delta^{18}$O results from an ongoing study of secondary clay minerals preserved in the upper Chicxulub peak-ring (Units 2 and 3). In particular, we examine the context of the clays within the post-impact hydrothermal system, and the isotopic information they preserve on the fluids that affected this part of the structure.

Our initial analyses revealed these clays to be texturally and chemically diverse, belonging predominantly to the smectite group, and displaying a range of sizes (Figure 1), crystallinity and chemical composition (i.e., Fe-Mg vs Al-K-rich varieties) [3]. Following up on this work, we have expanded our study to include samples from other intervals, examination of other clay size fractions, and additional techniques to determine: (1) whether any zonation or transitions are preserved through all subunits, so that we may form a more complete cross section through the upper peak-ring; (2) whether different size clay fractions in these lithologies are mineralogically and isotopically distinct, and (3) the temperatures and fluid sources within the hydrothermal system, focusing on conditions of clay mineral formation.

**Methods:** All analyses were performed using facilities at the University of Western Ontario. Polished thin sections were examined using a JEOL JXA-8900 L electron microprobe with beam operating conditions of 15 kV. Following initial characterization, 13 samples of homogeneous melt-bearing breccias and of individual "glass" clasts were selected for clay mineral separation and powder X-ray diffraction (XRD), performed at the Laboratory for Stable Isotope Science (LSIS). Various particle sizes (i.e. <2, 2-0.2, and <0.2 $\mu$m) were separated by centrifugation. Aliquots of each were saturated with $Ca^{2+}$ and $K^{+}$, and then examined using a series of XRD scans in preferred orientation to identify the clay minerals [8,9,10]. XRD of randomly oriented samples was used to determine the b-parameters of the clay assemblages. XRD was performed using a high-brilliance Rigaku Rotaflex RU-200B series diffractometer, equipped with a rotating anode (Co K$\alpha$ source). Hydrogen and oxygen isotope analysis of the clay minerals was completed using conventional methods most recently summarized by Huggett et al. (2017) [11].

**Results:** Smectite is consistently the dominant clay mineral group present through Units 2 and 3, in both the 2 to 0.2 $\mu$m and <0.2 $\mu$m size fractions. There are changes, however, in the smectite octahedral cation site occupancy from trioctahedral to dioctahedral through the peak-ring that correlate with increased host rock porosity [12].

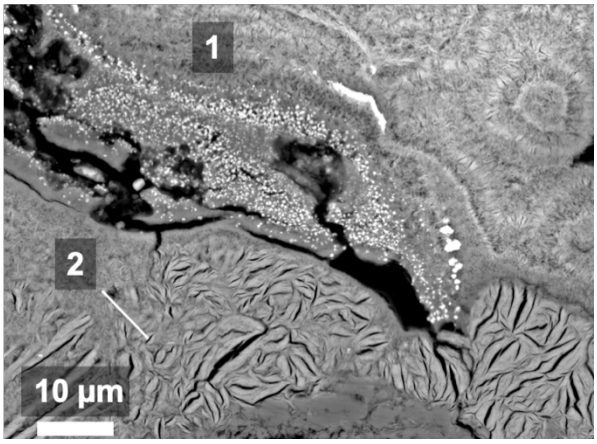


Figure 1: Backscattered electron (BSE) image of altered glass clast in melt-bearing impact breccia (Unit 2A) showing different sized smectites, in-situ. Label (1) indicates the very fine clays and (2) the larger, more crystalline size fraction.

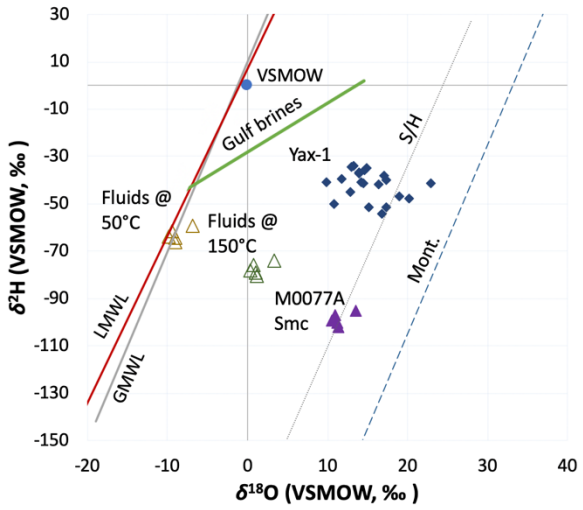


Figure 2: Summary of initial subset of $\delta^{18}O$ and $\delta^{2}H$ results obtained for the <2 $\mu$m size fraction of five samples (M0077A: Smc), and their respective calculated fluid compositions at 50°C and 150°C; this positions the putative fluids in $\delta$ - $\delta$ space in a region that could indicate mixing among meteoric water, seawater and basinal brine endmembers as well as rock-organic-water interaction. These are compared to the results for bulk silicate analysis in Yaxcopoil-1 (Yax-1) [13]. Also shown are Local and Global Meteoric Water Lines (LMWL and GMWL, respectively), Gulf brines [15, 16, 17], the supergene-hydrothermal line (S/H) after Sheppard and Gilg (1996) [14] and the montmorillonite weathering line (Mont.) after Savin and Epstein (1970) [18].

Initial $\delta^{18}O$ and $\delta^{2}H$ results for the <2 $\mu$m size fraction of 5 samples from Units 2A (~629, 636, 639 and 663 mbsf) and 2C (~714 m below sea floor) are shown in Figure 2. Our $\delta^{18}O$ results lie within the lower end of range obtained from bulk silicate analysis of the Yaxcopoil-1 core [13], which sampled the annular trough surrounding the peak ring. Direct comparison, however, is not possible as the size fractions and overall mineral compositions analyzed were different from this study. Our $\delta^{2}H$ results are much lower (by ~50 ‰) than those obtained for the Yaxcopoil-1 core.

**Discussion:** Our initial isotopic results suggest moderate hydrothermal temperatures (50–150°C) and an enigmatic source of fluids (Fig. 2); the corresponding fluids calculated based on the lower limit of the supergene-hydrothermal temperature range are also shown for reference. These results remain open to interpretation at this time. We note, however, that these data likely do not reflect a single, unmodified fluid endmember (e.g. seawater, meteoric water, basinal brines) but rather may be a product of mixing of multiple fluid reservoirs and/or rock-water-organic interactions. For example, previous fluid inclusion studies of early-formed post-impact quartz veins within the underlying Cretaceous sedimentary rocks in the Yaxcopoil-1 core suggested that hydrocarbon migration and maturation was driven by impact-induced hydrothermal activity [19]. Similar processes may have affected clay-forming fluids in the peak-ring.

Forthcoming $\delta^{18}O$ and $\delta^{2}H$ analyses of an expanded sample set should provide more conclusive information about the fluid types and temperatures associated with formation of the various clay size fractions through the core. For example, the isotopic compositions of different clay size fractions within the peak-ring may record distinct fluid events [20], either because of different conditions of crystallization or differential susceptibility to post-formational isotopic exchange. For example, smaller, more poorly crystallized clay size fractions (<0.2, <0.1 $\mu$m) have a higher surface area to-volume ratio than their larger, better crystallized counterparts, making them more susceptible to isotopic exchange. Additional XRD characterization, explored more thoroughly in Simpson et al. (2019) [21], will also provide more complete information on the variations in clay mineralogy through these intervals, particularly those sections expressing dioctahedral versus trioctahedral zonation in smectite composition. Integration of the mineralogical and isotopic datasets should provide a fuller description of the range of fluid chemistries and temperatures during smectite formation in the Chicxulub peak-ring.

**References:** [1] Morgan, J. V. et al. (2016) *Science,* 354, 878–882. [2] Gulick, S. P. S. et al. (2018) *Proc. Of the IODP Vol. 364*. [3] Simpson, S. L. et al. (2018) *LPSC XLIX*, abstract #2518. [4] Kring, D. A. et al. (2017) *LPSC XLVIII,* abstract #1212. [5] Feuillie, C. (2013) *GCA,* 120, 97-108. [6] Cockell, C. C. et al. (2010) *Chemical Geology 279, 17-30*. [7] Brindley, G.W. and Brown, G., Eds., Crystal Structures of Clay Minerals and Their X-Ray Identification, *Mineralogical Society*, 305-356. [8] Libbey, R. et al. (2013) *Clays and Clay Minerals*, 61, 204-217. [9] Ignasiak et al. (1983) *Fuel*, 62, 353-362. [10] McKay, J. et al. (2013) *Clays and Clay Minerals,* 61, 440-460. [11] Huggett, J. A. et al. (2017) *Clay Minerals*, 52, 25-50 [12] Christeson, G. L. et al. (2018) *Earth and Planetary Science Letters*, 495, 1–11. [13] Zurcher, L. et al. (2005) *GSA Special Paper*, 384. [14] Sheppard, S. and Gilg, H. (1996) *Clay Minerals*, 31, 1-24 [15] Moldovanyi, E. P et al. (1993) *GCA*, 57, 2083-2099. [16] Knauth, P. L. et al. (1980) *JGR*, 85, 4863-4871. [17] Clayton, R. et al. (1966) *JGR,* 71, 3869-3882. [18] Savin, S. and Epstein, S. (1970) *GCA,* 34, 25-42. [19] Luders and Rickers (2004) *MAPS*, 19, 1187-1197. [20] Yeh, H. (1980) *GCA*, 44, 341-352. [21] Simpson, S. L. et al. (2019) *LPSC L, this conference*.